Anionic Oligomerization of Acrylonitrile Molecules Initiated by Intracluster Electron Transfer from Alkali Metal Atoms: Photoionization Mass Spectrometry of $M(CH_2{=}CHCN)_n$ (M = Li, Na, and K)

Keijiro Ohshimo, Fuminori Misaizu,* and Koichi Ohno

Department of Chemistry, Graduate School of Science, Tohoku University, Aramaki, Aoba-ku, Sendai 980-8578, Japan

Received: August 23, 1999; In Final Form: October 28, 1999

We investigated the photoionization mass spectrometry of clusters of alkali metal atoms (M = Li, Na and K) solvated with acrylonitrile (AN; $CH_2{=}CHCN$) molecules to obtain the information on size-dependent stability of the clusters. In the photoionization mass spectra of $M_m(AN)_n$, strong ion signals were observed at $M^+(AN)_3$. The $M^+(AN)_n$ (n = 6 and 9) ions were also clearly observed as magic numbers in the mass spectra of M = Na and K. By comparison with the mass spectrum of cluster ions formed by ion−molecule reactions in the cluster source, these magic numbers were found to be due to the stability of neutral clusters. These results are explained by the intracluster electron transfer from an alkali metal atom to AN molecules followed by anionic oligomerization. The results of the calculation for Na(AN) based on density functional theory also supports this consideration.

I. Introduction

It is well-known that polymerization reaction of vinyl compounds is caused by electron-donative species in the condensed phase.[1] For example, alkali metals act as an initiator of such a polymerization reaction. In this reaction, known as anionic polymerization, electron transfer from the reaction initiator causes a cleavage of the C=C bond of a vinyl molecule and produces an anion radical. This radical reacts with another molecule to produce a propagated anion radical, which sequentially reacts with other molecules. In general, such a reaction proceeds efficiently for the vinyl species that have electron-withdrawing groups such as cyano (−CN) group or halogen. For example, the anionic polymerization of acrylonitrile (AN; $CH_2{=}CHCN$), that is, monosubstituted ethylene by CN group, is readily initiated by the electron transfer from alkali metal in the condensed phase, and polyacrylonitrile (PAN) is formed through the reaction.

The anionic oligomerization of vinyl compounds also was studied in the gas phase using a flowing afterglow apparatus by McDonald and Chowdhury.[2,3] In their study, the ion−molecule reaction between CH_2CN^- ion and AN was used for the initial step of the oligomerization.[2] The oligomer, $NCCH_2{-}(AN)_n{-}AN^-$, is produced up to n = 3 in this reaction. Intracluster anionic oligomerization of vinyl compounds also was investigated extensively by Tsukuda and Kondow (TK) using the molecular beam method combined with electron attachment techniques.[4−6] They observed that the $(AN)_3^-$ ion is produced efficiently in the collisional electron transfer from high-Rydberg rare gas atoms. The $(AN)_n^-$ ions were also investigated by photodissociation spectroscopy,[7] collision-induced dissociation,[8] and photoelectron spectroscopy.[9] Through these studies, they concluded that the intracluster oligomerization is initiated by electron attachment to $(AN)_3$ and forms a stable anion radical that has a ring structure.

The metal−AN system was actively investigated by experiments and theoretical calculations during the past decade[10−13] in relation to the coating of metal surfaces with PAN films, which should serve to protect the surfaces from corrosion. Studies of the electrochemically initiated polymerization of AN on metal surfaces found that highly uniform and adherent thin PAN films can be formed on a substrate of particular metals (Ni and Cu), whereas the PAN films can easily peel off on others (Al and Zn).[10,11] Calculations were also performed for the complexes between the AN molecule and transition metal atoms (Ni, Cu, and Zn).[11] On the basis of density functional theory (DFT), stable structures were found for Ni(AN) and Cu(AN), but not for Zn(AN). These calculations are consistent with their experimental results.[11]

On the other hand, the gas-phase clusters of an alkali metal atom solvated with polar solvent molecules have also been studied extensively[14] by experiments and theoretical calculations. For example, photoionization mass spectrometry of the clusters of an alkali atom solvated with water, $M(H_2O)_n$ (M = Li,[15] Na,[16−18] and Cs[19]), and with ammonia, $M(NH_3)_n$ (M = Li,[15,20] Na,[18,21] and Cs[19]), has been investigated by several groups. Of interest in these studies is the mechanism of electron transfer from an alkali metal atom to solvent molecules, which causes formation of solvated electrons in polar solvents. The authors' group has also studied photoionization of the clusters of Li and Na atoms with simple organic molecules, such as CH_3CN (acetonitrile)[22] and $(CH_3)_2CO$ (acetone),[23] which have π electrons. In the study of the calculation of $M((CH_3)_2CO)$, the intracluster electron transfer is explained by the overlap between a valence orbital of the metal atom and an antibonding π orbital (π^*_{CO}) of acetone.[23] However, decisive evidence of the intracluster electron transfer from an alkali atom to the solvent molecules has not been obtained experimentally so far.

In this study, we have investigated the clusters of alkali metal atoms (Li, Na, and K) solvated with AN by photoionization mass spectrometry. The possibilities of the electron transfer and

* Corresponding author. E-mail: misaizu@qpcrkk.chem.tohoku.ac.jp.

10.1021/jp992968r CCC: $19.00 © 2000 American Chemical Society
Published on Web 12/31/1999

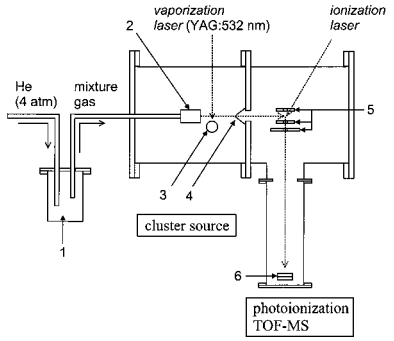

Figure 1. Schematic diagram of the experimental setup: (1) acrylonitrile sample in the reservoir; (2) pulsed valve (0.8-mm orifice diameter); (3) rotating and translating metal rod (6-mm diameter); (4) conical skimmer (1-mm diameter); (5) acceleration grids for ions; (6) dual microchannel plate.

of the intracluster reactions are discussed from the size distributions observed in the mass spectra. From another measurement of the mass spectrum of cluster ions formed by ion−molecule reactions in the cluster source, we have discussed the origins of the size distributions of clusters appeared in the photoionization mass spectra. We have compared the results obtained in this study with previous studies of $(AN)_n^-$ ions and have discussed the intracluster anionic oligomerization initiated by electron transfer from the alkali metal atom. The quantum chemical calculations on the basis of DFT have also been performed to get further insight into the interactions between the alkali atom with AN molecules.

II. Experimental Section

These experiments were performed by using an apparatus reported previously.[22] The experimental setup for measuring the photoionization mass spectra of the neutral clusters is shown in Figure 1. We used two-stage differentially pumped chambers consisting of a cluster source and a Wiley−McLaren type time-of-flight mass spectrometer (TOF-MS).[24] The pressures of the source and the TOF-MS chambers were maintained at about 2×10^{-5} and 7×10^{-7} Torr during measurements.

The clusters of alkali metals solvated with AN, $M_m(AN)_n$ (M = Li, Na, and K), were produced by a pickup source[16,17] consisting of a combination of laser vaporization[25] and pulsed supersonic expansion. A mixture gas of helium (Nihon Sanso, 99.9999% pure) and AN (Tokyo Kasei, 99% pure) was expanded from a pulsed valve (General Valve, series 9, orifice diameter 0.8 mm) with a stagnation pressure of 4 atm. The mixing ratio of AN in He gas was estimated to be 3% from the vapor pressure of AN. The second harmonic of a Nd:YAG laser (Lumonics, HY-400, 532 nm) was focused onto a metal rod (diameter, 6 mm), which was rotated and translated for stabilizing the vaporizing conditions, placed at about 10 mm downstream from the nozzle. The prepared cluster beam was collimated by a conical skimmer (throat diameter, 1 mm) positioned about 30 mm downstream from the nozzle. The liquid nitrogen cold trap was mounted near the skimmer to avoid clogging it with alkali metal.

Single photon ionization of the neutral clusters, $M_m(AN)_n$, was performed by irradiation with a pulsed laser beam at 230 mm downstream from the nozzle. The fourth harmonic of Nd:YAG laser (Lumonics, HY-400, 266 nm) or the frequency-doubled output of a dye laser (Lumonics, HD-300) pumped by a Nd:YAG laser (Spectra-Physics, GCR-150−10) was used as a photoionization light source. To avoid multiphoton ionization processes, the fluence of the ionization laser was kept under 4 mJ/cm^2 during the measurement. The timings of the valve opening and both the vaporization and ionization laser irradiation were optimized by a digital delay/pulse generator (Stanford Research, DG535). The cluster ions formed by photoionization were accelerated to about 2.3 keV by static electric fields applied to acceleration grids. The accelerated ions were introduced to a field-free tube of 550 mm length. The mass-separated ions were detected by a dual microchannel plate (Hamamatsu, F1552−21S), and the output signals were stored and averaged by a digital storage oscilloscope (LeCroy, 9344C). The data stored in the oscilloscope were sent to a personal computer (NEC, PC-9801DA) via a GPIB computer interface.

Along with the measurements above, mass spectra of the cluster ions nascently formed in the cluster source were also measured. Cluster ions were generated by reactions between alkali metal ions made by laser vaporization and neutral AN clusters in the expansion region of the free jet. These cations were introduced to the acceleration region of TOF-MS and were accelerated to about 1.0 keV by pulsed electric fields generated by a high-voltage pulse generator (DEI, GRX-1.5K−E). The timing of acceleration field pulse with respect to the others was also optimized by the digital delay/pulse generator.

The sample rod of lithium (Wako, 99% pure) was made from lump under argon atmosphere to avoid the reaction with nitrogen or water. The sample rod of sodium (Nacalai, 99% pure) and potassium (Aldrich, 99.5% pure) were made in the same way under nitrogen atmosphere.

III. Calculations

The quantum chemical calculations for the geometry optimization of AN and Na(AN) were performed to examine the extent of intracluster electron transfer. All calculations in this study were carried out by using a DFT program of Gaussian 94.[26] The 6-31+G* basis set and the B3LYP functional[27] were used in these calculations. The calculated bond lengths of AN molecule showed excellent agreement (within 0.006 Å) with those determined by microwave spectroscopy.[28] Moreover, we made a natural population analysis[29] for the optimized structures to estimate the charge distributions within clusters. Natural population analysis is reliable to estimate the charge distributions in molecules of high ionic character such as those containing the alkali metal atoms. The electron distribution in the singly occupied molecular orbital (SOMO) of Na(AN) was also calculated to discuss the intracluster electron transfer.

IV. Results and Discussion

A. Size Distribution in Photoionization Mass Spectrum of $Na_m(AN)_n$. Figure 2a shows a typical mass spectrum obtained by one-photon ionization of $Na_m(AN)_n$ by irradiation with a laser beam of 4.66 eV. In this figure, the series of cluster ions of $Na^+(AN)_n$ is mainly observed up to $n = 9$. The peaks caused by the dissociation of one or more hydrogen atoms of AN molecules are observed in the vicinity of $Na^+(AN)$ and $Na^+(AN)_3$, however, the contribution of the dissociative cluster ions are small in the whole mass range as shown in the figure. Several intensity anomalies (magic numbers) in the $Na^+(AN)_n$ series are found in this mass spectrum. The intensity of $Na^+(AN)_3$ is about seven times greater than that of $Na^+(AN)_2$. In addition, the intensity gaps between $Na^+(AN)_n$ and $Na^+(AN)_{n+1}$ are also observed at $n = 6$ and 9. Although not shown in this figure, the ion signal of $Na^+(AN)_{12}$ is also observed intensely with respect to adjacent n ions. This magic-number behavior at $n = 3k$ ($k = 1-4$) is independent of the wavelength of the ionization laser in the region between 4.66 and 5.58 eV. The peak of Na_2^+-

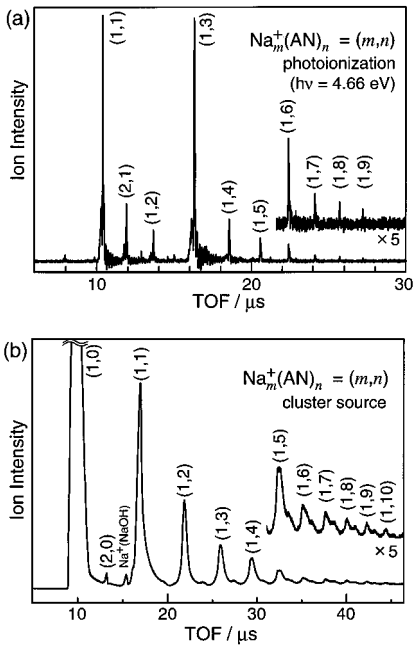

Figure 2. Typical mass spectra of $Na_m^+(AN)_n$ produced by (a) photoionization ($h\nu = 4.66$ eV) of neutral $Na_m(AN)_n$, and by (b) ion−molecule reaction in the cluster source. (m,n) denotes $Na_m^+(AN)_n$ ion.

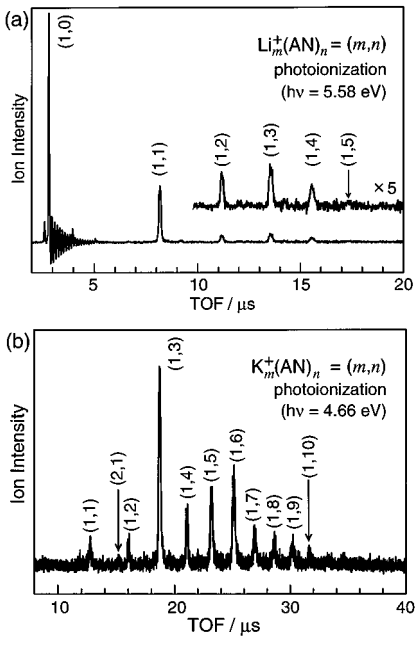

Figure 3. Photoionization mass spectra of (a) $Li_m(AN)_n$ and (b) $K_m(AN)_n$. Ionization energies are 5.58 and 4.66 eV for a and b, respectively. (m,n) denotes $M_m^+(AN)_n$ (M = Li and K) ions.

(AN) is also observed, whereas, the peaks of larger sodium clusters solvated with AN, such as $Na_m^+(AN)_n$ ($m \geq 3$), are not observed. This tendency is common to the pickup source because there is no channel for growing metal clusters in front of the pulsed valve. In the photoionization mass spectroscopy of $Na_m(H_2O)_n$ using the pickup source, the series of $m = 2$ is reported to be weakly observed along with that of $m = 1$, and those of $m \geq 3$ are not observed.[17]

In a photoionization mass spectrum of neutral clusters of solvated metal atoms (MS_n, M = metal, S = solvent molecule), there are at least three factors to be considered which cause magic numbers: (1) the size distribution of each n of neutral MS_n clusters in the beam, which depends on the stability of neutral clusters generated in the cluster source, (2) the ionization efficiency of neutral clusters at certain photon energy for ionization, and (3) the probability of evaporation processes of M^+S_n ions, $M^+S_n \rightarrow M^+S_{n-m} + mS$, in the acceleration region after photoionization, which in turn depends on the stability of cluster ions. Among these, we can assume that the ionization efficiency is almost constant or at least not sensitively dependent on n for all clusters in the present mass spectrum, because the photon energy is much higher than ionization thresholds of these clusters. Therefore, possibility 2 can be ruled out. If the evaporation processes take place efficiently after photoionization, relatively stable ions tend to be populated by evaporation from less stable ions, and as a result, the n-dependent stability of ions will be reflected on the size distribution in the photoionization mass spectrum. To determine the origin of magic numbers at $n = 3k$ in this study, we also measured the mass spectrum of the $Na_m^+(AN)_n$ ions nascently formed by ion−molecule reaction in the cluster source as shown in Figure 2b. In this mass spectrum, it is expected that the observed size distribution depends on the stability of ions. The series of cluster ions of $Na^+(AN)_n$ is observed up to $n = 10$, in addition to Na^+ and Na_2^+ ions. Although a possibility of containing dissociative ions in this mass spectrum exists, we have assigned these peaks to $Na^+(AN)_n$ ions tentatively because of low mass resolution due to pulsed extraction and Coulomb broadening. The intensities of ions decrease monotonically with increasing n, and the magic-number behavior at $n = 3k$ in Figure 2a is not observed in this mass spectrum. Therefore, we can assume that the stability of $Na^+(AN)_n$ ions formed in the source does not depend sensitively on n, and that the magic numbers are related to the nature of neutral $Na_m(AN)_n$ clusters. In addition, in the ionization with a photon energy of 3.84 eV, the same magic-number behavior is found at $n = 3$. This photon energy is only 0.21 eV above the ionization thresholds for $Na(AN)_n$ ($2 \leq n \leq 6$) as shown in Section IV.C. Therefore, the appearance of the magic number is little affected by the evaporation process after photoionization (possibility 3). After all, the magic numbers at $n = 3k$ observed in the photoionization mass spectrum are concluded to be due to the size distribution of neutral $Na_m(AN)_n$ clusters (possibility 1).

B. Intracluster Electron Transfer in $M_m(AN)_n$ (M = Li, Na, and K). To know the origin of the magic numbers at $n = 3k$ in Figure 2a, we also measured the photoionization mass spectra of clusters containing other alkali metal atoms, $Li_m(AN)_n$ and $K_m(AN)_n$, as shown in Figure 3. The photon energy was 5.58 eV for one-photon ionization of $Li_m(AN)_n$ (Figure 3a) and 4.66 eV for that of $K_m(AN)_n$ (Figure 3b). The series of $Li^+(AN)_n$ and $K^+(AN)_n$ ions are observed up to $n = 5$ and 10, respectively. Exactly the same periodical magic numbers at $n = 3k$ [$k = 1$ for $Li^+(AN)_n$, $k = 1{-}3$ for $K^+(AN)_n$] are found in these spectra. These periodical magic-number behaviors common to the alkali metal−AN clusters cannot be explained by their stabilities of geometrical structures, which are expected to be sensitively dependent on the radii of solvated metal atoms. The atomic radii of these alkali metal atoms are much different from each other: those of Li, Na, and K atoms are 1.52, 1.86, and 2.27 Å, respectively.[30] As a result, these magic numbers can be attributed to the electron configuration of the metal atom. In other words, the ns valence electron of the alkali metal atom plays a crucial role in the formation of magic number clusters.

It is well-known that the electron transfer from alkali metal initiates the anionic polymerization reaction of AN in the condensed phase. Also in $M_m(AN)_n$, the alkali metal atom is expected to act as an electron donor to the AN cluster. It is informative to compare the present results with the detailed

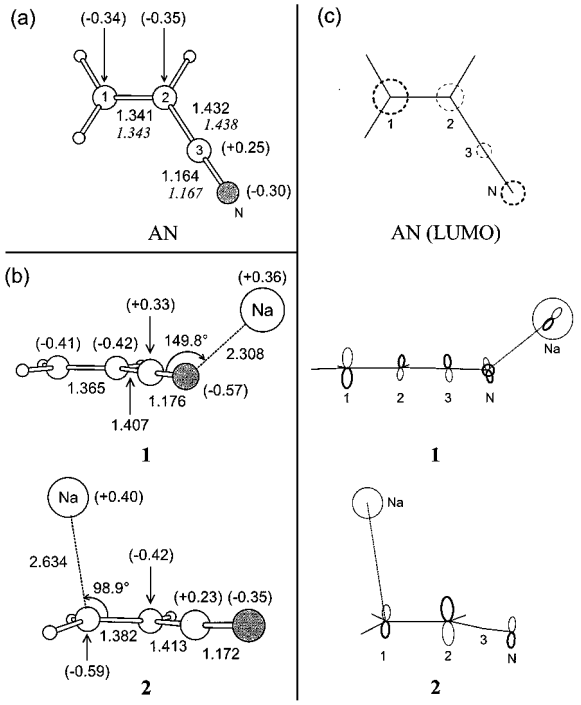

Figure 4. Calculated structures and natural charges (in parentheses) of: (a) AN and (b) Na(AN). The bond lengths of AN determined by microwave spectroscopy[28] are also shown in italics. (c) Schematic representation of the LUMO for AN and the SOMO for each isomer of Na(AN). Valence s orbitals and in-plane p orbitals are shown by solid circles and pairs of ellipses, respectively. Out-of-plane component of p orbitals is shown by dashed circles. Signs of orbital coefficients are indicated by the thickness of the curves, and the size of circle and ellipse is proportional to the coefficient of each atomic orbital.[31]

studies of the stability of $(AN)_n^-$ ions by Kondow and co-workers.[5,7−9] Throughout their studies, $(AN)_n^-$ ($n = 3$ and 6) ions are stable among $(AN)_n^-$ series. They concluded that these stable species are produced by intracluster oligomerization after electron attachment to $(AN)_n$, which is related with anionic polymerization in condensed phase. The magic numbers observed in their studies coincide with those in the present photoionization experiments. Therefore, the common magic numbers at $n = 3k$ in the photoionization mass spectra of $M_m(AN)_n$ (M = Li, Na, and K) indicate the presence of intracluster electron transfer from alkali metal atom to AN, which is followed by anionic oligomerization.

To get further insight into the intracluster electron transfer between the alkali metal atom and AN, we have optimized the structures of Na(AN) based on DFT (B3LYP/6-31+G*). Structures obtained for neutral AN molecule and for two isomers of Na(AN) (designated as **1** and **2**) are shown in Figure 4. Calculated bond lengths and natural charges are shown in the figure along with atomic labeling. The position of the Na atom with respect to AN is different between the two isomers. The structure of isomer **2** resembles that of Cu(AN), which is obtained in the calculation based on DFT within the local spin density approximation.[11] Binding energies with respect to separated Na and AN, ΔE_1, are evaluated to be 8.0 and 1.4 kcal/mol for **1** and **2**, respectively.[32] In both isomers, natural charges on the Na atom are approximately +0.4, and thus, the electron of the Na atom is transferred partly to AN. The structures of AN in both Na(AN) isomers also reveal that the intracluster electron transfer partly takes place. The lengths of $C_1{=}C_2$ and $C_3{\equiv}N$ bonds in both isomers are approximately 1−3% longer than that of free AN. On the other hand, the length of $C_2{-}C_3$ bond is approximately 2% shorter. These changes in bond lengths can be explained clearly by consideration of the electron distribution in the SOMO of Na(AN). In the SOMO of **1**, as shown in Figure 4c, the population of antibonding over the $C_1{=}C_2$ and $C_3{\equiv}N$ bonds, which is the lowest unoccupied molecular orbital (LUMO) of AN, is large because the valence electron of Na atom is transferred to AN. Therefore, the antibonding nature of the SOMO causes the elongation of the bond lengths. On the other hand, the resulting bonding nature of the $C_2{-}C_3$ bond shortens the bond length. The situation is almost the same in **2**, except that the transferred electron is mainly localized over the $C_1{=}C_2$ bond. Thus, the length of the $C_1{=}C_2$ bond in **2** becomes longer than that in **1**. In isomer **1**, the $Na{-}N{-}C_3$ bond angle is 149.8°. If we consider only the overlap between the valence 3s orbital of Na atom and π^*_{CN} orbitals, the favorable bond angle will be 90°. It is expected that the deviation of $Na{-}N{-}C_3$ bond angle from 90° is attributed to the overlap between Na3p and N2s orbitals. In isomer **2**, the $Na{-}C_1{-}C_2$ bond angle is 98.9°. This angle is also reasonable because, if the Na atom is located at the symmetrical position over the $C_1{=}C_2$ bond, this type of isomer will be unstable because of the antibonding character between Na3s and $C_2$2p orbitals. In these isomers, calculated values of Mulliken spin density of C_2 atom are −0.14 and +0.17 for **1** and **2**, respectively. In general, the positive spin density of C_2 atom is preferable to anionic polymerization. Thus isomer **2** is expected to be important in anionic oligomerization despite its lower stability than isomer **1**. We have also calculated the optimized structures of Li(AN) and found that the electron of the Li atom is also partly transferred to AN.[33]

The vertical electron affinity of an AN molecule is determined to be a negative value, −0.21 eV, from electron transmission spectroscopy.[34] However, its adiabatic electron affinity is barely positive from the study of collisional electron transfer from a high-Rydberg rare gas atom by TK.[5,35] In their study, the $(AN)_3^-$ ion is produced more efficiently than $(AN)^-$.[5] Thus, it is expected that $(AN)_3$ can accept the excess electron more efficiently than the AN molecule. Present calculations reveal that the electron of the Na atom is partly transferred to AN in Na(AN), despite the poor ability of AN to accept the excess electron. Therefore, it is expected that in $Na(AN)_3$, a much larger part of the valence electron of the Na atom is transferred to $(AN)_3$ than in Na(AN). The theoretical calculation of $Na(AN)_3$ provides information about charge distribution. However, no available theoretical results have been obtained so far, probably because of the presence of many possible structural isomers.

C. Ring Formation in $M(AN)_3$ (M = Li, Na, and K). As discussed above, the common magic number at $M^+(AN)_3$ in the photoionization mass spectra of $M_m(AN)_n$ (M = Li, Na, and K) appears as a result of the intracluster anionic oligomerization reaction in $M(AN)_n$. In this reaction process, $(AN)_n^-$ is first produced by electron transfer from M, then is followed by oligomerization. If the oligomer formed from $(AN)_n^-$ has a linear-chain structure, which is typical in the bulk polymerization reaction, the smooth size distribution of $M^+(AN)_n$ will appear in the photoionization mass spectra. Therefore, to explain the magic number at $M^+(AN)_3$, we have to consider the stable structure especially for oligomerized $(AN)_3^-$. One assumption is that oligomerized $(AN)_3^-$ ion in $M(AN)_3$ has a ring geometry, which is assignable to an anion of 1,3,5-cyclohexanetricarbonitrile (CHTCN), as proposed by Kondow and co-workers. CHTCN is known as a stable species which can be prepared from 1,3,5-cyclohexanetricarboxylic acid by a four-step synthesis.[36] The synthesis of CHTCN using the anionic oligomerization of AN has not been reported in the condensed phase so

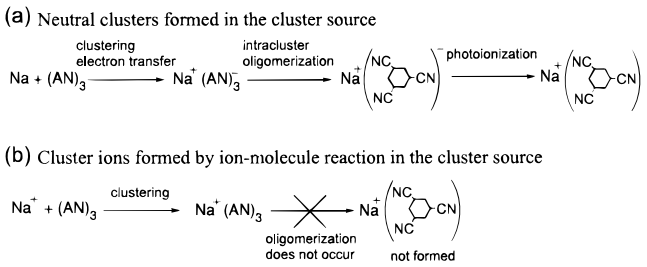

Figure 5. Reaction scheme of (a) neutral clusters formed in the cluster source and (b) cluster ions formed by ion−molecule reaction in the cluster source. The multiple collisions between $(AN)_n$ and He atoms actually occur in the reaction region.

TABLE 1: Determined Ionization Thresholds (I_{th}) of $Na(AN)_n$

n	I_{th} (eV)
0	5.14
1	4.04(18)
2−6	3.63(14)

far. However, trimethyl-substituted CHTCN, 2,4,6-trimethyl-1,3,5-cyclohexanetricarbonitrile, can be yielded by potassium-catalyzed trimerization of 2-butenenitrile.[37] In the study of $(AN)_n^-$,[5,7−9] it is concluded that the structure of oligomerized $(AN)_3^-$ ion is the CHTCN anion radical. A recent study[38] shows that the anion of synthesized CHTCN is certainly stable, that is, the adiabatic electron affinity is positive. After all the stable $Na(AN)_3$ is produced by the reaction scheme shown in Figure 5a. On the contrary, for the ions formed by ion−molecule reaction in the cluster source, $Na^+(AN)_3$ did not show special stability as shown in Figure 2b. This result is explained by the reaction scheme as shown in Figure 5b. In $Na^+(AN)_3$ formed in the source, the electron of Na^+ does not transfer to $(AN)_3$ because of the stable electron configuration of the Na^+ ion. Thus, the oligomerization reaction of $(AN)_3$ does not proceed after clustering. Therefore, the structure of $Na^+(AN)_3$ formed by photoionization of $Na(AN)_3$ is expected to differ from that of $Na^+(AN)_3$ formed by ion−molecule reaction.

We also determined the ionization thresholds (I_{th}) of $Na(AN)_n$ ($n \leq 6$) by measuring each photoion yield with scanning the photon energy of the ionization laser. The determined I_{th} values are listed in Table 1 along with the ionization energy of a Na atom.[39] I_{th} for larger clusters ($n \geq 7$) are not determined because of their low concentration in the cluster beam. The I_{th} value decreases monotonically with n for $n = 0-2$, whereas those for $2 \leq n \leq 6$ are constant at 3.63 eV as shown in Table 1. I_{th} is related to the binding energies (ΔE_n)[32] and their differences ($\Delta E_{n-1,n} = \Delta E_n - \Delta E_{n-1}$) of neutrals and ions by

$$I_{th}(n) = \Delta E_n[Na(AN)_n] - \Delta E_n[Na^+(AN)_n] + IP[Na] \quad (1)$$

$$I_{th}(n) = \Delta E_{n-1}[Na(AN)_n] + \Delta E_{n-1,n}[Na(AN)_n] - \Delta E_{n-1}[Na^+(AN)_n] - \Delta E_{n-1,n}[Na^+(AN)_n] + IP[Na] \quad (2)$$

where IP[Na] is the ionization energy of a Na atom. The obtained results of I_{th} suggests that $\Delta E_{n-1,n}$ of the cluster ions are higher than those of the neutral clusters for $n \leq 2$ and that those of the cluster ions are equal to those of the neutrals for $2 \leq n \leq 6$. From the discussion about the magic number in the neutral clusters, it is expected that I_{th} of $n = 3$ will be larger than that of $n = 2$. However, the I_{th} of $n = 3$ is the same value as that of $n = 2$ within experimental error. Therefore, the stability of the $Na^+(AN)_3$ ion relative to $Na^+(AN)_2$ is almost the same as that in the neutrals. This may be consistent with the fact that CHTCN is stable both in the neutral and anion species.[36,38] Similar behaviors of I_{th} are also reported for $M(H_2O)_n$ (M = Li,[15] Na,[16−18] and Cs[19]); the I_{th} value was constant for $n \geq 4$. In the recent theoretical study, this behavior of $M(H_2O)_n$ is explained by the stable ion-pair structure, $M^+(H_2O)_m(H_2O)_l(H_2O)_{n-m-l}^-$.[40] Therefore, the electron transfer from the metal atom to solvent clusters has a critical role in the I_{th} constancy, as in $M(AN)_n$. Although the comparison between these clusters is difficult because of the intracluster chemical reaction in $M(AN)_n$, it is still worth noting that the I_{th} tendency in $M(H_2O)_n$ is similar to that in $M(AN)_n$.

In the studies by TK, the electron attachment to $(AN)_3$ also tends to cause the elimination of the α-hydrogen atoms of AN molecules.[5,6] They explained that the excess energy, generated by the exothermic oligomerization (formation of CHTCN), causes the dissociation of the CH bond in AN. This explanation holds for the electron attachment process under collision-free condition. In the present photoionization mass spectra of $M_m(AN)_n$, as shown in Figures 2 and 3, the ion signals caused by the dissociation of AN are small, because the excess energy caused by the intracluster oligomerization of AN is removed by the multiple collision between He atoms and clusters. This is consistent with the character of our cluster source in which the multiple collision takes place in the region of cluster formation. It is concluded that the internal energy in $M(AN)_3$ become smaller than the energy needed to dissociate the CH bond as a result of efficient collisional relaxation processes in the region of production of $M(AN)_3$. For larger clusters, $M(AN)_n$ ($n \geq 4$), the excess energy is also removed by the evaporation of AN after the oligomerization in addition to collisional relaxation. This evaporation process results in the intense peaks at $M^+(AN)_3$ in the photoionization mass spectra.

D. Magic Numbers at $n = 6$ and 9 in $M(AN)_n$ (M = Na and K). In the photoionization mass spectra of $M_m(AN)_n$ (M = Na and K), the $M^+(AN)_6$ and $M^+(AN)_9$ ions are also observed as magic numbers in addition to $M^+(AN)_3$ (see Figures 2a and 3b). For $Na_m(AN)_n$, the $Na^+(AN)_{12}$ ion is also detected as a magic number. These magic numbers at $n = 3k$ ($k = 1-4$) show an interesting periodicity. This feature is also observed in the studies of stability of the $(AN)_n^-$ ions using the techniques of photodissociation[7] and collision-induced dissociation.[8] The $(AN)_3^-$ and $(AN)_6^-$ ions are produced dominantly by the photodissociation of $(AN)_n^-$ ($n \geq 7$) ions.[7] In the study of collision-induced dissociation of the $(AN)_n^-$ ions, the loss of the $(AN)_3$ unit takes place efficiently in collision of a Kr atom with $(AN)_n^-$ ($6 \leq n \leq 11$) ions.[8] From these results it is concluded that the $(AN)_n^-$ ($n \geq 6$) ions consist of a trimeric core ion, $(AN)_3^-$, solvated with stable trimer units $(AN)_3$ and AN monomer. For the explanation of the observed periodical magic numbers in the present study, it is expected that $M(AN)_n$ ($n \geq 6$) also contains a trimeric core ion, $(AN)_3^-$, and stable trimer units $(AN)_3$ and AN monomer. However, the mechanism of formation of plural stable trimer units $(AN)_3$ is unclear because only one electron takes part in the intracluster oligomerization in $M(AN)_n$. One assumption is that the electron of the oligomerized $(AN)_3^-$ transfers to another $(AN)_{n-3}$ site in $M(AN)_n$ and the intracluster oligomerization takes place to form another $(AN)_3^-$ ion. Our group is now modifying the cluster source to investigate the size distribution in the photoionization mass spectra of $M_m(AN)_n$ (M = Na and K; $m \geq 2$). In these systems containing more than one metal atom, plural electrons participate in the intracluster oligomerization in $M_m(AN)_n$ and the discussion about the formation of two or three trimer units $(AN)_3$ is expected to be clear. Our group is also studying the

other metal−AN clusters [for example, $Al_m(AN)_n$ and $Cu_m(AN)_n$] to get further insight into the mechanism of intracluster electron transfer followed by oligomerization of AN.

V. Conclusion

We have measured the photoionization mass spectra of clusters of alkali metal atom (M) solvated with acrylonitrile (AN). Intense ion signals assignable to $M^+(AN)_3$ ions are observed for M = Li, Na, and K. Magic numbers at $n = 6$ and 9 are also observed for $Na^+(AN)_n$ and $K^+(AN)_n$ ions. In comparison with the results of size distribution of $Na^+(AN)_n$ ions formed by ion−molecule reactions in the cluster source, the obtained magic numbers at $M^+(AN)_n$ ($n = 3$, 6, and 9) are found to be due to the stability of neutral clusters, $M(AN)_n$. From the results of the study of $(AN)_n^-$, the observed magic numbers at $n = 3$, 6, and 9 can be attributed to the species produced by intracluster oligomerization reaction after electron transfer from the metal atom to the AN clusters. The results of calculation for Na(AN) based on DFT also support this consideration. This is the first observation of the initial steps of the intracluster anionic oligomerization of AN initiated by electron transfer from neutral species. In other words, we have observed clear evidence of the intracluster electron transfer from alkali metal atoms as magic numbers at $n = 3$, 6, and 9 in the photoionization mass spectra of $M_m(AN)_n$.

Acknowledgment. The authors acknowledge Dr. Tatsuya Tsukuda for his helpful discussions on the stability of cluster anions containing AN molecules. We would like to thank Dr. Yuji Fukuda for providing us with his recent results on the study of the CHTCN anion. We also thank Dr. Yoshihiro Yamakita for his beneficial discussions on the structure of AN oligomer. The authors also thank the Computer Center of the Institute for Molecular Science for provision of the NEC HSP and HPC computer. This work was supported in part by a Grant-in-Aid for Scientific Research from the Japanese Ministry of Education, Science, Sports and Culture. K. Ohshimo is supported by the Research Fellowship of the Japan Society for the Promotion of Science for Young Scientists. F. Misaizu also acknowledges financial support from the Sumitomo Foundation, Kurata Foundation, and Mitsubishi Foudation.

References and Notes

(1) Tsuruta, T.; O'Driscoll, K. F., Eds. *Structure and Mechanism in Vinyl Polymerization*; Marcel Dekker: New York, 1969.
(2) McDonald, R. N.; Chowdhury, A. K. *J. Am. Chem. Soc.* **1982**, *104*, 2675.
(3) McDonald, R. N.; Chowdhury, A. K. *J. Am. Chem. Soc.* **1983**, *105*, 2194.
(4) Tsukuda, T.; Kondow, T. *J. Chem. Phys.* **1991**, *95*, 6989.
(5) Tsukuda, T.; Kondow, T. *J. Am. Chem. Soc.* **1994**, *116*, 9555.
(6) Tsukuda, T.; Kondow, T. *Chem. Phys. Lett.* **1992**, *197*, 438.
(7) Fukuda, Y.; Tsukuda, T.; Terasaki, A.; Kondow, T. *Chem. Phys. Lett.* **1996**, *260*, 423.
(8) Ichihashi, M.; Tsukuda, T.; Nonose, S.; Kondow, T. *J. Phys. Chem.* **1995**, *99*, 17354.
(9) Fukuda, Y.; Tsukuda, T.; Terasaki, A.; Kondow, T. *Chem. Phys. Lett.* **1995**, *242*, 121.
(10) Lécayon, G.; Bouizem, Y.; Le Gressus, C.; Reynaud, C.; Boiziau, C.; Juret, C. *Chem. Phys. Lett.* **1982**, *91*, 506.
(11) Fredriksson, C.; Lazzaroni, R.; Brédas, J. L.; Mertens, M.; Jérôme, R. *Chem. Phys. Lett.* **1996**, *258*, 356.
(12) Raynaud, M.; Reynaud, C.; Ellinger, Y.; Hennico, G.; Delhalle, J. *Chem. Phys.* **1990**, *142*, 191.
(13) Geskins, V. M.; Lazzaroni, R.; Mertens, M.; Jérôme, R.; Brédas, J. L. *J. Chem. Phys.* **1996**, *105*, 3278.
(14) Schulz, C. P.; Hertel, I. V. in *Clusters of Atoms and Molecules II*; Haberland, H., Ed., Springer-Verlag: Berlin-Heidelberg, 1994.
(15) Takasu, R.; Misaizu, F.; Hashimoto, K.; Fuke, K. *J. Phys. Chem. A* **1997**, *101*, 3078.
(16) Schulz, C. P.; Haugstätter, R.; Tittes, H. U.; Hertel, I. V. *Phys. Rev. Lett.* **1986**, *57*, 1703.
(17) Schulz, C. P.; Haugstätter, R.; Tittes, H. U.; Hertel, I. V. *Z. Phys. D* **1988**, *10*, 279.
(18) Hertel, I. V.; Hüglin, C.; Nitsch, C.; Schulz, C. P. *Phys. Rev. Lett.* **1991**, *67*, 1767.
(19) Misaizu, F.; Tsukamoto, K.; Sanekata, M.; Fuke, K. *Chem. Phys. Lett.* **1992**, *188*, 241.
(20) Takasu, R.; Hashimoto, K.; Fuke, K. *Chem. Phys. Lett.* **1996**, *258*, 94.
(21) Schulz, C. P.; Gerber, A.; Nitsch, C.; Hertel, I. V. *Z. Phys. D* **1991**, *20*, 65.
(22) Ohshimo, K.; Tsunoyama, H.; Yamakita, Y.; Misaizu, F.; Ohno, K. *Chem. Phys. Lett.* **1999**, *301*, 356.
(23) Tsunoyama, H.; Ohshimo, K.; Yamakita, Y.; Misaizu, F.; Ohno, K. *Chem. Phys. Lett.*, in press.
(24) Wiley: W. C.; McLaren, I. H. *Rev. Sci. Instrum.* **1955**, *26*, 1150.
(25) Dietz, T. G.; Duncan, M. A.; Powers, D. E.; Smalley, R. E. *J. Chem. Phys.* **1981**, *74*, 6511.
(26) Frisch, M. J.; Trucks, G. W.; Schlegel, H. B.; Gill, P. M. W.; Johnson, B. G.; Robb, M. A.; Cheeseman, J. R.; Keith, T.; Petersson, G. A.; Montgomery, J. A.; Raghavachari, K.; Al-Laham, M. A.; Zakrzewski, V. G.; Ortiz, J. V.; Foresman, J. B.; Cioslowski, J.; Stefanov, B. B.; Nanayakkara, A.; Challacombe, M.; Peng, C. Y.; Ayala, P. Y.; Chen, W.; Wong, M. W.; Andres, J. L.; Replogle, E. S.; Gomperts, R.; Martin, R. L.; Fox, D. J.; Binkley, J. S.; Defrees, D. J.; Baker, J.; Stewart, J. P.; Head-Gordon, M.; Gonzalez, C.; Pople, J. A. *Gaussian 94*, Revision E.2; Gaussian, Inc.: Pittsburgh, PA, 1995.
(27) Becke, A. D. *J. Chem. Phys.* **1993**, *98*, 5648.
(28) Fukuyama, T.; Kuchitsu, K. *J. Mol. Struct.* **1970**, *5*, 131.
(29) Reed, A. E.; Weinstock, R. B.; Weinhold, F. *J. Chem. Phys.* **1985**, *83*, 735.
(30) Emsley, J. *The Elements*, 3rd ed.; Oxford University Press: New York, 1998.
(31) Ohno, K.; Takano, S.; Mase, K. *J. Phys. Chem.* **1986**, *90*, 2015.
(32) The binding energies ΔE_n of these isomers can be evaluated by $-\Delta E_n = E[Na(AN)_n] - E[Na] - nE[AN]$ where $E[Na(AN)_n]$ is the total energy of $Na(AN)_n$; $E[Na]$ and $E[AN]$ are the total energies of Na atom and AN, respectively.
(33) Ohshimo, K.; Misaizu, F.; Ohno, K., Unpublished results.
(34) Jordan, K. D.; Burrow, P. D. *Acc. Chem. Res.* **1978**, *11*, 341.
(35) Tsukuda, T.; Kondow, T. *Chem. Phys. Lett.* **1991**, *185*, 511.
(36) Mayer, H. A.; Stöβel, P.; Fawzi, R.; Steimann, M. *Chem. Ber.* **1995**, *128*, 719.
(37) Shabtai, J.; Ney-Igner, E.; Pines, H. *J. Org. Chem.* **1975**, *40*, 1158.
(38) Fukuda, Y.; Ichihashi, M.; Terasaki, A.; Kondow, T.; Osoda, K.; Narasaka, K., private communication.
(39) Moore, C. E. *Atomic Energy Levels*; United States Department of Commerce, National Bureau of Standards: Washington, D. C., 1949; Vol. I.
(40) Tsurusawa, T.; Iwata, S. *J. Phys. Chem. A* **1999**, *103*, 6134.